Plasma Chem Plasma Process (2007) 27:1–11
DOI 10.1007/s11090-006-9034-2

ORIGINAL ARTICLE

Catalytic Effects of Metal-loaded Membrane-like Alumina Tubes on Ammonia Synthesis in Atmospheric Pressure Plasma by Dielectric Barrier Discharge

**Takanori Mizushima · Kazumi Matsumoto ·
Hironobu Ohkita · Noriyoshi Kakuta**

Received: 11 July 2006 / Accepted: 11 July 2006 /

Abstract Plasma synthesis of ammonia was studied at atmospheric pressure using a dielectric-barrier-discharge-plasma reactor equipped with a metal-loaded membrane-like alumina tube as a catalyst between the electrodes. Introducing the pure alumina into N_2–H_2 plasma resulted in an increase in the ammonia yield and the further improvement was achieved by loading the alumina with Ru, Pt, Ni, and Fe. These results clearly demonstrate the catalytic effects of the alumina and the metals in the plasma reaction. Temperature-programmed desorption and isotope exchange reaction of nitrogen revealed that plasma-excited N_2 molecules were subjected to dissociative adsorptions mainly on the alumina to form atomic N(a) (The suffix "(a)" denotes adsorbed species) species, which were converted into ammonia by H_2 plasma. A role of the metals is considered to be acceleration of ammonia formation by the reaction of the alumina-adsorbed N(a) atoms with plasma-activated hydrogen species.

Keywords Atmospheric pressure plasma · Plasma synthesis · Ammonia · Catalysis · Membrane-like alumina tube · Metal effects

1 Introduction

Due to high stability of N_2, its activation is the most important step in ammonia synthesis. In the Haber process, dissociative adsorption of N_2, which has been accepted to be the rate-determining step, is carried out on promoted iron catalysts at high temperatures and pressures [1, 2]. It is well known that efficient activation of N_2 at ambient conditions can be achieved by low-temperature plasmas; therefore, a number of studies on plasma synthesis of ammonia have been undertaken [3–13].

T. Mizushima (✉) · K. Matsumoto · H. Ohkita · N. Kakuta
Department of Materials Science, Toyohashi University of Technology, Tempaku-cho,
Toyohashi, Aichi 441-8580, Japan
e-mail: mizusima@tutms.tut.ac.jp

Electron impacts against N_2 molecules in plasma can generate a wide variety of excited species such as anions, cations, and radicals. In atmospheric-pressure silent discharge of N_2, the predominant excited species is metastable N_2* of the lowest triplet state ($A^3\sum_u^+$) [14]. It is produced by an electron transition from the bonding $1\pi_u$ orbital to the antibonding $1\pi_g$ orbital with a spin inversion, and hence the triple bond of N_2* is notably weakened. Nomura [11] has theoretically predicted some advantages of plasma excitation of N_2 in dissociative adsorption on catalysts and succeeding conversion to ammonia. In practice, he proved a switchover of the rate-determining step from the N_2 dissociation to the hydrogenation of nitrides formed on the stainless-steel reactor wall as a catalyst in ammonia production by the electron-cyclotron-resonance(ECR) plasma. More positive evidences for the plasma-induced dissociative adsorption of N_2 on metals have been given for Fe [8, 9], Mo[9], and Ru [15].

It has been also reported that plasma discharge allowed nondissociative chemisorption of N_2 on Al_2O_3. Kameoka et al. [16–18] observed IR bands approximately at 2260 and 2230 cm^{-1} after a N_2-plasma treatment of Al_2O_3 and assigned them to the N–N stretching of $N_2(a)$ molecules strongly chemisorbed on the Al_2O_3 surface with an end-on configuration. They also found that when Pt was present on Al_2O_3, the $N_2(a)$ molecules reacted with H_2 at room temperature to form NH_x (x = 1–3) species. Plasma synthesis of ammonia was also accelerated by MgO [12, 13]. These results clearly indicate that the metals and the oxides behaved as catalysts for ammonia formation by N_2–H_2 plasma.

We have previously designed a membrane-like alumina (MA) tube as a catalyst for a plasma reactor by dielectric barrier discharge [19]. The MA tube consisted of a gas-permeable alumina film prepared by the anodic oxidation technique, which had straight pores developed perpendicularly to the macroscopic surface. This plasma-catalytic reaction system is expected to improve the reaction efficiency via the following advantages: (1) the catalyst is placed at the center of the plasma zone, (2) plasma-activated molecules are forced into the catalyst pores, and hence have a high probability of contacting with the catalyst surface, and (3) it is easy to load the alumina membrane with catalytic active components. We demonstrated that the MA introduction into the N_2–H_2 plasma raised the ammonia yield and the Ru deposition on MA led to an additional increase, indicating significant interactions of plasma-excited N_2 and H_2 with the alumina and Ru. In the present work, we investigated catalytic effects of other metals, Pt, Ni, and Fe, and clarified the mechanism of ammonia formation on MA and Ru.

2 Experimental

2.1 Preparation of the MA tube and metal loading

The MA tube was prepared by anodic oxidation and chemical treatments of an aluminum tube (an outside diameter of 5 mm, a thickness of 0.25 mm, a length of 125 mm, and a purity of 99.5%). The details were described in the previous paper [19]. In short, a porous alumina layer was first formed on the inner wall of the aluminum tube by applying DC +100 V against a carbon-rod cathode (2 mm in diameter) installed through the tube with a flowing solution of 1 wt.% oxalic acid at 293 K. This processing was kept for 10 h. After washing with water, the tube was sealed at the both ends with Teflon tape and immersed in a 15 wt.% hydrochloric acid solution containing 0.1 mol/dm^3 copper(II) chloride to remove the external unanodized metal. The dense barrier layer at the bottom of the anodized film was then dissolved in a 25 wt.% phosphoric acid solution to puncture the pores through. For IR measurements, we also prepared a 20ϕ MA disk by anodizing an aluminum plate in the oxalic acid solution and then by the chemical treatments. A SEM observation elucidated that the MA films had straight pores of about 70 nm in diameter, which were developed independently of each other and perpendicularly to the macroscopic surface. The film thickness was approximately 100 μm. Loading the alumina with Ru, Pt, Ni, and Fe was carried out by immerging the MA tubes for 3 h in a saturated *n*-hexane solution of $Ru_3(CO)_{12}$, a 0.77 mmol/dm^3 aqueous solution of $H_2PtCl_6 \cdot 6H_2O$, and 0.1 mol/dm^3 aqueous solutions of $Ni(NO_3)_2 \cdot 6H_2O$ and $Fe(NO_3)_3 \cdot 9H_2O$, respectively. After calcination at 773 K for 4 h, the tubular catalyst was installed in the plasma reactor and then reduced with hydrogen at 673 K for 2 h before the reactions and the characterizations.

2.2 Ammonia synthesis by the plasma reactor equipped with the membrane-like catalyst

The dielectric-barrier-discharge-plasma reactor employed in this work had a triple-tubular structure as illustrated in Fig. 1. The core tube was the inner electrode of stainless steel (4 mm in outside diameter and 1 mm in thickness) on which three 1-mm holes were made at 30-mm intervals. The membrane-like catalyst as the second tube was mounted so as to cover the holes and fixed at the both ends with ceramic adhesive. These tubes were held in a quartz tube (6 mm in inside diameter and 1 mm in thickness) with plastic tube-fittings. After reducing the catalyst in a H_2 flow using a tubular electric furnace, a piece of aluminum foil (90 mm square) as the external electrode was wrapped around the quartz tube. Discharge plasma was generated by applying an AC voltage at 21.5 kHz between the inner and external electrodes with a power source (Logy Electric, LHV-13AC). The discharge voltage was monitored by an oscilloscope through a high-voltage probe. Gases were introduced from the end of the quartz tube and ejected from the core tube through the catalyst pores and the holes on the core tube. The products were analyzed by a gas chromatograph (Shimadzu, GC-8A) equipped with a 3-m column of HayeSep C 60/80.

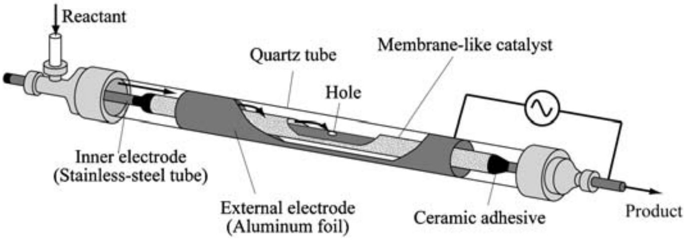

Fig. 1 A schematic diagram of the tubular plasma reactor equipped with the membrane-like catalyst

2.3 Temperature-programmed desorption (TPD)

We estimated nitrogen species adsorbed on the membrane-like catalyst through N_2-TPD. The catalyst was reduced at 673 K for 2 h in the reactor and then evacuated at the same temperature for 1 h. N_2 plasma was generated at 93.3 kPa and 4.5 kV for 5 min. After evacuation using a turbomolecular pump below 1×10^{-5} Pa at room temperature for 40 min, the catalyst temperature was raised to 773 K at a rate of 10 K/min. N_2 released from the catalyst was monitored by a quadrupole mass spectrometer (Anelva, AQA-200).

2.4 Infrared (IR) spectroscopy

Adsorbed N_2 molecules were identified by IR spectroscopy using a glass *in-situ* cell equipped with CaF_2 windows, an external heater, and two stainless-steel electrodes. The disk-shaped catalyst hung with a copper wire was reduced and evacuated in the cell under the same conditions as those for TPD. The sample was then moved between the electrodes and exposed to plasma in 93.3 kPa of N_2 by applying an AC voltage at 40 W. IR spectra were obtained by a JASCO FT/IR-410 spectrometer with an MCT detector at a resolution of 4 cm^{-1}.

2.5 Isotope exchange reaction (IER) of nitrogen

IER between $^{14}N_2$ and $^{15}N_2$ was carried out to verify dissociative adsorption of N_2 on the catalyst. After the reduction and the evacuation, a mixture of 50% $^{14}N_2$ and 50% $^{15}N_2$ was introduced into the reactor at an initial pressure of 26.7 kPa. A change in the ratio of $^{14}N_2$:$^{14}N^{15}N$:$^{15}N_2$ by plasma discharge at 4.5 kV was continuously monitored by the quadrupole mass spectrometer.

3 Results

3.1 Effects of the membrane-like catalysts on plasma synthesis of ammonia

Ammonia synthesis was carried out in the plasma reactors with and without the membrane-like catalysts at ambient temperature and pressure. Under all conditions employed in this work, NH_3 was exclusively produced and hydrazine, N_2H_4, was not detected. Figure 2 shows the NH_3 yield at a H_2/N_2 molar ratio of 3 and a total flow amount of 30 cm^3/min as a function of effective alternating voltage (rms). The amount of NH_3 formed in the blank reactor slightly increased with input voltage up to 3.5 kV but leveled off at higher voltages. The yield at 4.5 kV was 1.6×10^{-5}mol/min, which corresponded to a N_2 conversion of 2.4%.

As is evident from Fig. 2, the NH_3 formation was accelerated at each input voltage by introducing the metal-free MA into the N_2–H_2 plasma. At 4.5 kV, the produced amount was 1.5 times as large as that for the blank. Loading MA with the metals resulted in a further increase in the NH_3 yield. For all of the metals, the yield increased with input voltage up to 4.5 kV. The electric power consumptions, which were 51 ± 3, 65 ± 3, 84 ± 5, 106 ± 6, and 127 ± 9 W at 2.5, 3.0, 3.5, 4.0, and 4.5 kV, respectively, remained nearly unaffected by MA and the metals. It is, therefore, concluded that the alumina and the metals behaved as catalysts for the NH_3

Fig. 2 Effects of the input voltage and the membrane-like catalysts in the plasma synthesis of ammonia at a H_2/N_2 molar ratio of 3 and a total flow amount of 30 cm^3/min: ◆, blank; ◇, MA; ▲, Fe/MA; △, Ni/MA; ●, Pt/MA; ○, Ru/MA

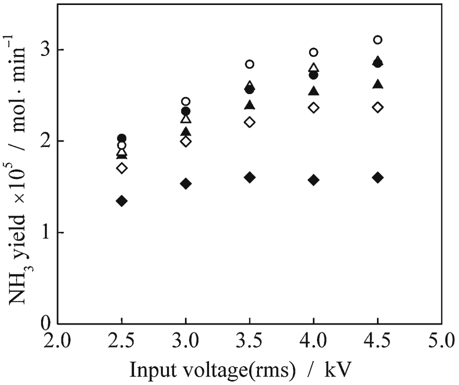

production in N_2–H_2 plasma. A sequence of the catalytic activities at 4.5 kV was Ru/MA > Ni/MA ≈ Pt/MA > Fe/MA > MA. It should be noted that, although Ni and Pt have low activities for thermal synthesis of NH_3, they showed relatively high yields in the plasma synthesis, suggesting differences in the reaction mechanism and the rate-determining step.

Effects of the H_2/N_2 molar ratio on the NH_3 formation at a discharge voltage of 4.5 kV and a total flow amount of 30 cm^3/min are illustrated in Fig. 3. The catalyst-mounted reactors exhibited higher yields than the blank reactor at each H_2/N_2 ratio. The NH_3 yield increased with increasing H_2/N_2 ratio up to 5 in the absence of the catalyst but it decreased at higher H_2/N_2 ratios when the catalyst was present. The gas composition at which the maximum yield was obtained depended on the catalysts: the optimum H_2/N_2 ratio for MA, Fe/MA, and Ru/MA was 3, which is the stoichiometric value for NH_3 synthesis, but the maximum for Pt/MA and Ni/MA was shifted to a H_2/N_2 ratio of 2.

In order to elucidate the roles of the alumina and the metals in the plasma-catalytic synthesis of NH_3, we carried out the following tests for Ru/MA that showed the highest activity, as well as the metal-free MA. First, the catalyst was exposed to N_2 plasma at a flow amount of 40 cm^3/min and a discharge voltage of 4.5 kV for 5 min. After sweeping the reactor with a 40-cm^3/min flow of H_2 for 0–3 min without

Fig. 3 Effects of the H_2/N_2 molar ratio and the membrane-like catalysts in the plasma synthesis of ammonia at an input voltage of 4.5 kV and a total flow amount of 30 cm^3/min: ◆, blank; ◇, MA; ▲, Fe/MA; △, Ni/MA; ●, Pt/MA; ○, Ru/MA

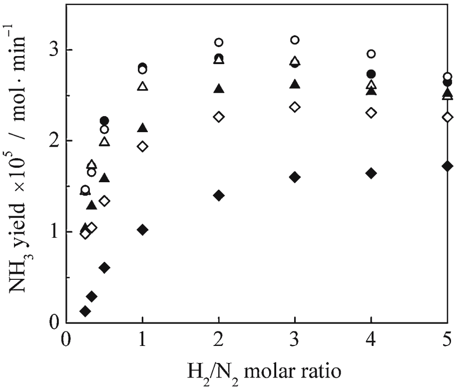

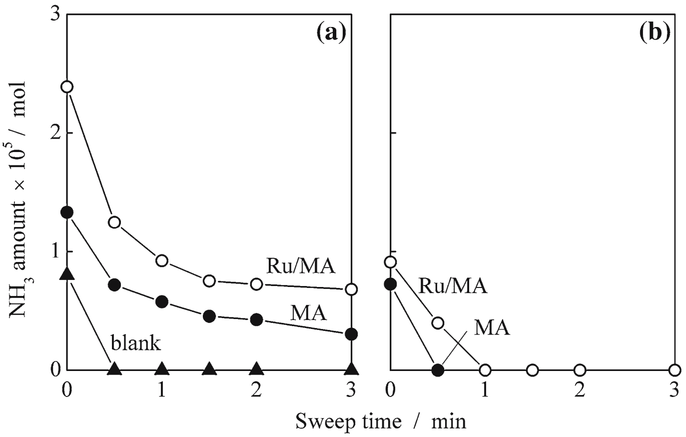

Fig. 4 Amount of NH_3 produced (**a**) by H_2 plasma after N_2 plasma and (**b**) by N_2 plasma after H_2 plasma as a function of the sweep time between the both plasma treatments

discharge, the plasma was generated in H_2 at 4.5 kV for 5 min. NH_3 produced during the H_2 plasma was temporarily trapped at the liquid nitrogen temperature and then quantitated by the gas chromatograph. In Fig. 4a, the produced amount of NH_3 is plotted as a function of the H_2 sweep time. Since N_2 in the reactor was completely replaced by H_2 within 1 min, it follows that NH_3 produced after sweeping for 1.5 min and more was derived from adsorbed nitrogen species. No product was detected for the blank reactor, suggesting that very little nitrogen was adsorbed on the reactor wall and the inner-electrode surface. On the other hand, in the presence of MA and Ru/MA, NH_3 was generated by the H_2 plasma after a sweep time of 1.5 min and the amount scarcely decreased at longer sweep times. NH_3 produced in the Ru/MA-mounted reactor after the 3-min sweep was approximately twice as much as that for the metal-free MA. It was also confirmed that NH_3 was not formed by a H_2 flow without discharge. These results indicate that the nitrogen was chemisorbed on the membrane-like catalyst and hydrogenated by plasma-excited hydrogen to NH_3.

We also attempted the NH_3 production in the reverse sequence, i.e. H_2 plasma, sweeping with N_2, and then N_2 plasma. The results are shown in Fig. 4b. No detectable amount of NH_3 was observed after the complete replacement of H_2 in the reactor equipped with MA and Ru/MA. Consequently, it is speculated that the adsorbed nitrogen rather than hydrogen is essential for the NH_3 formation on the catalysts.

3.2 Characterization of the adsorbed nitrogen species

N_2-TPD measurements were made to characterize the nitrogen species adsorbed on MA and Ru/MA. After the pretreatments, mass peaks were observed at $m/z = 14$ and 28 as well as 16, 17, and 18 for residual H_2O. When the non-plasma-treated catalyst was heated up to 773 K at a rate of 10 K/min, the peak intensity at m/z 28 was slightly reduced with a constant intensity ratio of the peaks at m/z 14–28. This demonstrates that the 28 m/z peak was not due to CO emitted from the catalyst but due to residual N_2 in the system.

The open triangles and circles in Fig. 5 represent N_2-TPD spectra of MA and Ru/MA, respectively, treated by N_2 plasma for 5 min. There is not much difference between the two. The catalysts began to release N_2 approximately at 500 K and the desorbed amount continued to increase up to 773 K. As was expected, N_2 desorption was not detected when the catalyst was exposed to N_2 without discharge or when the catalyst was absent (rhombuses in Fig. 5), indicating that the strong chemisorption of nitrogen on the catalyst surface was induced by the plasma excitation of N_2.

Effects of H_2 plasma on the adsorbed nitrogen species were also investigated by TPD. After the N_2 plasma, the catalyst was exposed to H_2 plasma for 5 min and evacuated at room temperature for 40 min. Changes in the N_2-TPD spectra of MA and Ru/MA are shown by the filled triangles and circles, respectively, in Fig. 5. The amount of N_2 released from Ru/MA was markedly reduced in the temperature range of 500–700 K by the H_2-plasma treatment, whereas a decrease in the desorbed amount was observed over 600 K for the Ru-free MA. The ratios of the integrated signal intensities after to before the H_2 plasma were 0.85 and 0.55 for MA and Ru/MA, respectively. Taking into consideration the results shown in Fig. 4a, it is concluded that Ru promoted emission of the adsorbed nitrogen as NH_3.

We carried out FT-IR measurements to identify the nitrogen species adsorbed on the catalysts. MA and Ru/MA showed very intense absorption bands in the range of 1800–1300 cm^{-1}. These bands were attributable to oxalate species incorporated into the alumina films during the anodization [20, 21]. Figures 6a and b illustrate IR spectra ranging from 2300 to 2100 cm^{-1} for MA and Ru/MA, respectively. For the pretreated catalysts (Spectra a1 and b1), we observed two peaks at 2276 and 2131 cm^{-1}, which were also due to the anodic films. The spectra were not changed by a N_2 admission without discharge (Spectra a2 and b2). When plasma was generated through MA in N_2 for 2 h, two small absorption bands appeared approximately at 2238 and 2210 cm^{-1} in Spectrum a3. These are assigned to N–N stretching modes of molecular N_2(a) chemisorbed on different sites of MA with an end-on configuration according to Kameoka et al. [16–18] who observed two peaks at about 2260 and 2230 cm^{-1} in the IR spectrum of Al_2O_3 exposed to plasma-excited N_2. The smaller

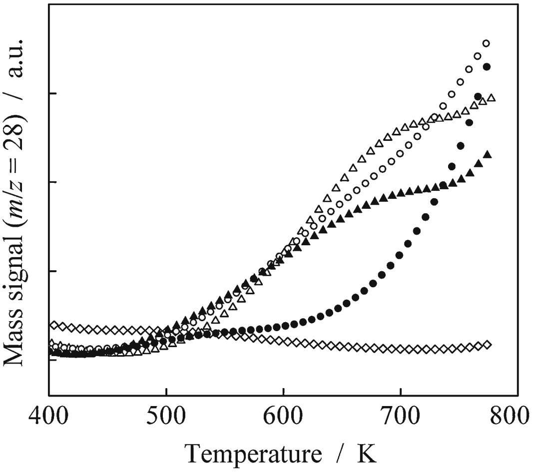

Fig. 5 N_2-TPD spectra from MA (△▲) and Ru/MA (○●) exposed to N_2 plasma (open symbols) and to H_2 plasma after N_2 plasma (filled symbols). The blank reactor (◇) was also examined for comparison

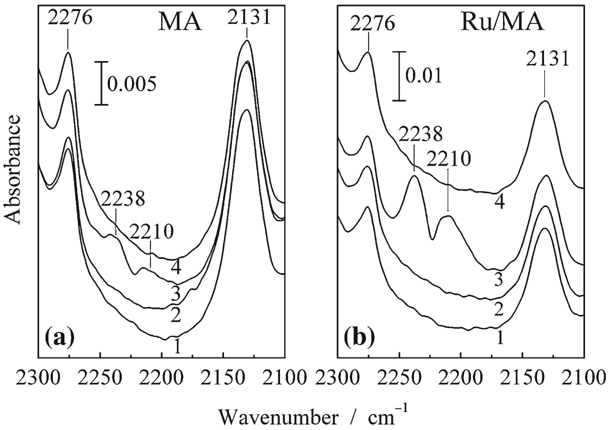

Fig. 6 IR spectra of (a) MA and (b) Ru/MA: (1) after the pretreatments; (2) after N_2 admission; (3) after N_2 plasma for 2 h; (d) after evacuation at room temperature

wavenumbers observed in this study may be caused by the incorporation of oxalate anions into the alumina.

Similar IR peaks due to N_2(a) species were also detected in Spectrum b3 for Ru/MA, but they were approximately 7 times as intense as those for MA, implying the presence of other adsorption sites. Kubota and Aika [22] have reported that N_2(a) on 2 wt% Ru/Al_2O_3 reduced at 873 K showed an IR peak at 2214 cm^{-1} with a shoulder at 2268 cm^{-1}. The latter band was observed even at a reduction temperature of 673 K, but the former peak appeared above 773 K and was shifted to smaller wavenumbers with increasing temperature. From these results, they assigned the peaks at 2268 and 2214 cm^{-1} to the N–N stretching modes of N_2(a) adsorbed on the partially oxidized Ru and the metallic Ru, respectively. Consequently, the IR peaks at 2238 and 2210 cm^{-1} in Spectrum b3 are most likely due to N_2(a) molecules adsorbed on the Ru sites as well as MA.

Evacuating MA and Ru/MA at room temperature resulted in complete disappearance of the IR bands due to N_2(a) as shown in Spectra a4 and b4, indicating that the molecular N_2(a) was loosely attached to the catalysts unlike the nitrogen species released over 500 K in the N_2-TPD. This also means that NH_3 formed by exposing the N_2-plasma-treated catalysts to H_2 plasma (Fig. 4a) was not derived from the N_2(a) species; therefore, other adsorbed nitrogen, N(a) atoms, must be present on the catalyst surface.

To make sure of it, we performed the nitrogen IER, $^{14}N_2 + {}^{15}N_2 = 2{}^{14}N^{15}N$, in the plasma reactor with and without the membrane-like catalysts. Fig. 7 shows compositional changes in the reactor with discharge time. The reaction occurred even in the blank reactor, and hence the N_2 dissociation took place in the gaseous plasma and/or on the reactor surfaces such as the stainless-steel electrode and the quartz tube. By introducing the membrane-like catalysts, the formation rate of $^{14}N^{15}N$ and the consumption rates of $^{14}N_2$ and $^{15}N_2$ were approximately doubled. No effect of Ru on the IER rate was observed, suggesting that plasma-excited N_2 was subjected to dissociative adsorption on the alumina rather than on Ru. Taking into account the results in Figs. 4a and 5, we concluded that the alumina surface was covered with the tightly-adsorbed N(a) atoms, which were hydrogenated to NH_3 by H_2 plasma.

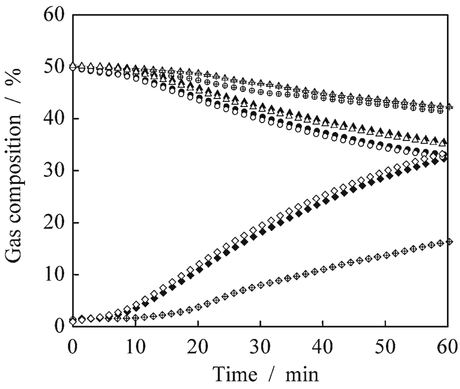

Fig. 7 Changes in the concentrations of $^{14}N_2$(⨹▲△), $^{14}N^{15}N$(◈◆◇), and $^{15}N_2$(⊕●○) in the isotope exchange reaction between $^{14}N_2$ and $^{15}N_2$ (1:1) by plasma:⨹◈⊕, blank; ▲◆●, MA; △◇ ○, Ru/MA

4 Discussion

4.1 Ammonia formation in the plasma reactor without the membrane-like catalyst

Since NH_3 was obtained even in the blank reactor as shown in Figs. 2 and 3, we must first allow for the production routes of NH_3 other than the surface reactions on the membrane-like catalyst. It has been previously substantiated that NH_3 formation in the plasma phase of N_2–H_2 was progressed by reactions of NH radicals with hydrogen [4, 6, 7]. Kiyooka and Matsumoto [10] have also elucidated that large amounts of NH_x radicals were produced on the surface of the stainless-steel wall of the ECR chamber as a catalyst. Similar catalytic effects of the metallic electrodes and the reactor walls made of glass and metal have been reported [4, 11]. Accordingly, in the present work, it is a good guess that NH_3 was formed by two reaction pathways in the blank reactor: the gas phase reactions via NH radicals and the surface reactions on the quartz reactor wall and the stainless-steel electrode. If the former is the major route, raising the plasma power is expected to increase the amount of NH radicals and thereby to enhance the NH_3 yield. On the other hand, an increase in the surface reactions is probably restricted by the very small surface areas of the reactor wall and the inner electrode. Figure 2 indicates that the NH_3 yield for the blank did not increase with increasing voltage over 3.0 kV, and hence that the surface reaction was the dominant process for the NH_3 formation.

4.2 Ammonia formation on the membrane-like catalysts and a role of metals

The reaction tests evidently demonstrated the catalytic effects of the alumina and the metals in the plasma synthesis of NH_3. Plasma-excited N_2 was dissociated and adsorbed on the catalyst to form N(a) atoms, which were desorbed by heating over 500 K in vacuum. Molecular N_2(a) species were also confirmed to be on the catalyst, but their adsorptions were so loose as to be desorbed by evacuation at room temperature.

Since the N_2-TPD profile and the IER rate for Ru/MA were almost equivalent to those of the pure MA, it is considered that the dissociative adsorption of N_2 was free of the influence of Ru, and hence the atomic N(a) spices were chemisorbed chiefly

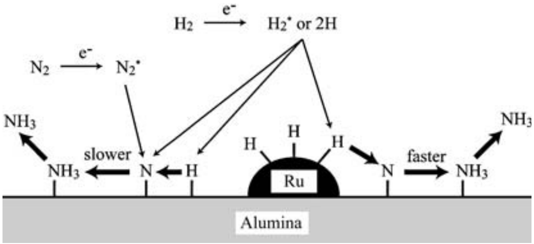

Fig. 8 A schematic diagram of the NH_3 formation pathway on Ru/MA in N_2–H_2 plasma

on MA. The N(a) species were not hydrogenated by a H_2 flow at room temperature but were converted to NH_3 by plasma discharge in H_2, suggesting that they reacted with plasma-activated hydrogen species such as H atoms and excited H_2^* molecules. Kunimori et al. [15] have found that plasma-excited N_2 was subjected to dissociative adsorption on ruthenium black and the resulting N(a) atoms showed a TPD peak with a top approximately at 543 K. In addition, they were hydrogenated to NH_3 by an atmospheric H_2 flow at room temperature. The evident differences in the TPD profile and the reactivity with hydrogen support our conclusion that the N(a) species existed on the alumina rather than on Ru.

Despite a lack of contributions to the N_2 dissociation, Ru showed significant catalytic effects on the NH_3 formation in N_2–H_2 plasma. Although the amount of the N(a) atoms on the alumina remained nearly unaffected (Fig. 5), the amount of NH_3 produced by exposing the N(a) atoms to H_2 plasma was appreciably increased by Ru (Fig. 4a). These facts lead to a speculation that Ru accelerated hydrogenation of the N(a) atoms on the alumina to NH_3. Figure 8 illustrates our suggestions as to formation routes of NH_3 on the membrane-like catalyst. Atomic N(a) species are produced on the alumina through the dissociative adsorption of N_2^* molecules excited by electron impacts. Plasma discharge also generates activated hydrogen species such as H atoms and H_2^* molecules. These hydrogen species react with the N(a) atoms directly or via adsorption on the alumina to form NH_3. When Ru is present on the alumina, NH_3 is also produced by reactions of the N(a) atoms with H(a) atoms on Ru. This reaction is relatively faster and thereby a lager amount of NH_3 is obtained.

The proposed reaction pathway suggests that the rate-determining step is not the dissociative adsorption of N_2 but the hydrogenation of the N(a) species as was pointed out by Nomura [11]. Consequently, the NH_3 yield is expected to depend on hydrogenation behaviors of the supported metals. This may produce the reaction result in Fig. 3 that the optimum H_2/N_2 ratio for Pt/MA and Ni/MA was different from that for Ru/MA and Fe/MA.

5 Conclusions

The membrane-like alumina placed in N_2–H_2 plasma showed an apparent catalytic effect for NH_3 formation. Plasma-excited N_2 was dissociated and adsorbed on the alumina to form atomic N(a) species, which reacted with H atoms or activated H_2^* molecules to NH_3. When the metals were present on the alumina, hydrogenation of the N(a) species was accelerated to increase the NH_3 yield. These results indicate the effectiveness of the membrane-like catalyst for an atmospheric-pressure plasma reactor by dielectric-barrier discharge.

Acknowledgment This study was supported in part by Grant-in-Aid for Scientific Research from the Japan Society for Promotion of Science.

References

1. Stoltze P (1995) In: Nielsen A (ed) Ammonia, catalysis and manufacture. Chap. 2, Springer-Verlag, Berlin, pp 17–102
2. Ozaki A, Aika K (1981) In: Anderson JR, Boudaet M (eds) Catalysis — science and technology, vol. 1, Chap. 3, Springer-Verlag, Berlin, pp. 87–158
3. Eremin EN, Mal'tsev AN, Belova VM (1971) Russ J Phys Chem 45:205
4. Yin KS, Venugopalan M (1983) Plasma Chem Plasma Process 3:343
5. Touvelle M, Munoz Licea JL, Venugopalan M (1987) Plasma Chem Plasma Process 7:101
6. Uyama H, Matsumoto O (1989) Plasma Chem Plasma Process 9:13
7. Uyama H, Matsumoto O (1989) Plasma Chem Plasma Process 9:421
8. Uyama H, Nakamura T, Tanaka S, Matsumoto O (1993) Plasma Chem Plasma Process 13:117
9. Tanaka S, Uyama H, Matsumoto O (1994) Plasma Chem Plasma Process 14:491
10. Kiyooka H, Matsumoto O (1996) Plasma Chem Plasma Process 16:547
11. Nomura O (1983) Technocrat 16:29
12. Sugiyama K, Akazawa K, Oshima M, Miura H, Matsuda T, Nomura O (1986) Plasma Chem Plasma Process 6:179
13. Mingdong B, Xiyao B, Zhitao Z, Mindi B (2000) Plasma Chem Plasma Process 20:511
14. Gherardi N, Gouda G, Gat E, Ricard A, Massines F (2000) Plasma Sources Sci Technol 9:340
15. Kunimori K, Osumi M, Kameoka S, Ito S (1992) Catal Lett 16:443
16. Kameoka S, Ito S, Kunimori K 1993) In: Inui T, Fujimoto K, Uchijima T, Masai M (eds) Proceedings of the third International Conference on Spillover, Elsevier, Amsterdam, pp. 257–260
17. Kameoka S, Kuriyama T, Ito S, Kunimori K (1993) Hyomen Kagaku 14:623
18. Kunimori K, Kuriyama T, Ito S, Kameoka S (1994) Jpn J Appl Phys 33:4195
19. Mizushima T, Matsumoto K, Sugoh J, Ohkita H, Kakuta N (2004) Appl Catal A: General 265:53
20. Yamamoto Y, Baba N (1983) Thin Solid Films 101:329
21. Xu T, Zhao J, Cheng J, Dang H (1997) J Trace Microprobe Tech 15:521
22. Kubota J, Aika K (1994) J Phys Chem 98:11293